Available online at www.sciencedirect.com
ScienceDirect
International Journal of Pharmaceutics 346 (2008) 1–9
INTERNATIONAL JOURNAL OF PHARMACEUTICS
www.elsevier.com/locate/ijpharm

Alginate–magnesium aluminum silicate composite films: Effect of film thickness on physical characteristics and permeability

Thaned Pongjanyakul [a,*], Satit Puttipipatkhachorn [b]

[a] *Faculty of Pharmaceutical Sciences, Khon Kaen University, Khon Kaen 40002, Thailand*
[b] *Department of Manufacturing Pharmacy, Faculty of Pharmacy, Mahidol University, Bangkok 10400, Thailand*

Received 1 March 2007; received in revised form 24 April 2007; accepted 29 May 2007
Available online 2 June 2007

Abstract

The different film thicknesses of the sodium alginate–magnesium aluminum silicate (SA–MAS) microcomposite films were prepared by varying volumes of the composite dispersion for casting. Effect of film thickness on thermal behavior, solid-state crystallinity, mechanical properties, water uptake and erosion, and water vapor and drug permeability of the microcomposite films were investigated. The film thickness caused a small change in thermal behavior of the films when tested using DSC and TGA. The crystallinity of the thin films seemed to increase when compared with the thick films. The thin films gave higher tensile strength than the thick films, whereas % elongation of the films was on the contrary resulted in the lower Young's modulus of the films when the film thickness was increased. This was due to the weaker of the film bulk, suggesting that the microscopic matrix structure of the thick films was looser than that of the thin films. Consequently, water uptake and erosion, water vapor permeation and drug diffusion coefficient of the thick films were higher than those of the thin films. The different types of drug on permeability of the films also showed that a positive charge and large molecule of drug, propranolol HCl, had higher lag time and lower diffusion coefficient that acetaminophen, a non-electrolyte and small molecule. This was because of a higher affinity of positive charge drug on MAS in the films. The findings suggest that the evaporation rate of solvent in different volumes of the composite dispersion used in the preparation method could affect crystallinity and strength of the film surface and film bulk of the microcomposite films. This led to a change in water vapor and drug permeability of the films.

Keywords: Sodium alginate; Magnesium aluminum silicate; Film; Microcomposite; Mechanical property; Permeability

1. Introduction

Sodium alginate (SA) is a sodium salt of alginic acid, a naturally occurring non-toxic polysaccharide found in marine brown algae. Alginate has been widely used as food and pharmaceutical additives, such as a tablet disintegrant and gelling agent (Kibbe, 2000). It contains two uronic acids, α-L-guluronic and β-D-mannuronic acids, and is composed of homopolymeric blocks and blocks with an alternating sequence (Draget, 2000). Gelation occurs by cross-linking of the uronic acids with divalent cations, such as calcium ion. This phenomenon has been used to prepare drug loaded calcium–alginate beads (Badwan et al., 1985; Sugawara et al., 1994; Takka et al., 1998). A cross-linked film between SA and divalent ions has also been prepared and investigated some physical properties, such as mechanical properties (Remuñán-López and Bodmeier, 1997), water vapor transmission (Remuñán-López and Bodmeier, 1997) and drug permeability (Julian et al., 1988; Aslani and Kennedy, 1996; Remuñán-López and Bodmeier, 1997).

Magnesium aluminum silicate (MAS) is a mixture of montmorillonite and saponite clays (Kibbe, 2000), which have a layered structure. Each layer is constructed from tetrahedrally coordinated silica atoms fused into an edge-shared octrahedral plane of either aluminium hydroxide or magnesium hydroxide (Alexandre and Dubois, 2000; Kibbe, 2000). The layer structures of clays could be separated when they were hydrated in water. Once MAS is hydrated the weakly positive edges are attracted to the negatively charged faces. The attraction of face to edge of these colloidal layers creates a three-dimensional colloidal structure throughout the dispersion, which exhibited a thixotropic property (Zatz and Kushla, 1989). The charges on the layers of MAS lead to an interaction with anionic polymer,

* Corresponding author. Tel.: +66 43 362092; fax: +66 43 202379.
E-mail address: thaned@kku.ac.th (T. Pongjanyakul).

0378-5173/$ – see front matter © 2007 Elsevier B.V. All rights reserved.
doi:10.1016/j.ijpharm.2007.05.058

such as xanthan gum (Ciullo, 1981) and carbomer (Ciullo and Braun, 1991), which resulted in viscosity synergism.

Recently, MAS was used to improve rheological properties of SA gel (Pongjanyakul et al., 2005a). The flow type of the SA gels was shifted from Newtonian to pseudoplastic with thixotropic property and drug release from the composite gels was sustained. This led to a study of physicochemical properties of the SA–MAS composite films. The SA and MAS could form a microcomposite film and improved mechanical properties, and retarded water uptake and drug permeability of the films were reported (Pongjanyakul et al., 2005b). Moreover, plasticized microcomposite films were developed by incorporating hydrophilic small molecules, namely glycerin and polyethylene glycol 400. The added plasticizers caused changes in thermal behavior, matrix structure, mechanical properties, and permeability on water vapor and drugs (Pongjanyakul and Puttipipatkhachorn, 2007).

For development of film used in pharmaceutics, film thickness is one of parameters that could affect physicochemical properties of the films, such as gas permeability (Shishatskii et al., 1996; McCaig and Paul, 2000) and mechanical properties (Ononokpono and Spring, 1988; Jansson and Thuvander, 2004). Thus, it is interesting that physicochemical properties of polymer–clay composite films may be changed due to the thickness of film, which is prepared by casting/solvent evaporation method. This leads to the aims of the present study on preparation of the different thicknesses of the SA–MAS microcomposite films by varying volumes of the composite dispersion for casting. Physical properties of the films such as thermal behavior, solid-state crystallinity, mechanical properties, water uptake and erosion, and water vapor permeation were investigated. Moreover, permeability of the films on different types of drug was examined as well. Additionally, surface morphology and internal structure of the composite films were compared with the SA films by using scanning electron microscopy (SEM).

2. Materials and methods

2.1. Materials

Low viscosity grade of sodium alginate (SA, viscosity of 2% solution at 25 °C: 250 cps) was purchased from Sigma Chemical Company (MO, USA). MAS (Veegum® HV) was obtained from R.T. Vanderbilt Company, Inc. (Norwalk, CT, USA). Acetaminophen (ACT) and propranolol HCl (PPN) were purchased from Praporn Darsut Ltd. (Bangkok, Thailand). Other reagents used were of analytical grade and used as received.

2.2. Preparation of films

Films were prepared using casting/solvent evaporation technique, which have been previously reported (Remuñán-López and Bodmeier, 1997; Pongjanyakul et al., 2005b). SA (2 g) was dispersed in distilled water using homogenizer for 5 min, whereas MAS (2 g) was prehydrated with hot water for 15 min. The MAS dispersion was mixed into the SA dispersion using homogenizer for 5 min, and was then adjusted the volume with distilled water to 200 ml. The SA–MAS dispersion was kept for full hydration at room temperature overnight. Then, 100, 200 or 300 ml of the composite dispersion was poured onto plastic plate (15 cm × 20 cm), allowed to evaporate at 50 °C, and the durations for drying were approximately 12, 24 or 36 h, respectively. The composite films were peeled off and kept in a desiccator (40 ± 2% RH). Moreover, the SA film without MAS was also prepared by using 200 ml of 1% (w/v) SA dispersion and then the preparation was proceeded as described above.

2.3. Characterization of films

2.3.1. Thickness of films

Thickness of dry and wet films was measured in 10 places using microprocessor coating thickness gauge (Minitest 600B, ElektroPhysik, Germany). The dry films (4 cm × 4 cm) were cut and placed on a control plate. The probe, which was connected with the measurement gauge and calibrated using a standard film, gently moved downward to touch on the film and the thickness of film was then measured. The films were subsequently placed in a small beaker containing 0.1 M HCl, which was shaken occasionally in water bath at 37.0 ± 0.5 °C. The samples were taken and blotted to remove excess water. The thickness of wet films was immediately determined following the procedure mentioned above.

2.3.2. Scanning electron microscopic studies

Surface morphology and cross-section of films were observed using SEM. Samples were mounted onto stubs, sputter coated with a gold in a vacuum evaporator, and photographed using scanning electron microscope (Jeol Model JSM-5800LV, Tokyo, Japan).

2.3.3. Differential scanning calorimetry (DSC)

DSC thermograms of samples were recorded using a differential scanning calorimeter (DSC822, Mettler Toledo, Switzerland). Each sample (2–3 mg) was accurately weighed into a 40 μl aluminum pan without an aluminum cover. The measurements were performed over 30–350 °C at a heating rate of 10 °C/min.

2.3.4. Thermogravimetric analysis (TGA)

TGA thermograms of samples were measured using a thermogravimetric analyzer (TGA/SDTA851, Mettler Toledo, Switzerland). Each sample (3–4 mg) was accurately weighed into a 150 μl alumina oxide crucible. The measurements were conducted over the range of 30–800 °C at a heating rate of 10 °C/min.

2.3.5. Powder X-ray diffractometry

Powder X-ray diffraction measurements were performed on a powder X-ray diffractometer (Philips PW3710 mpd control, The Netherlands). The measurement conditions were a Cu radiation generated at 30 kV and 20 mA as X-ray source, angular of 1–35°(2θ) and step angle of 0.02°(2θ)/s.

2.3.6. Mechanical properties of films

The mechanical properties of films were measured using a Texture Analyzer (TA.XT plus, Surrey, UK). The films were cut into 10 cm × 1 cm strips, and kept in a chamber (55% RH, 25 °C) for 3 days before testing (ASTM, 2002; Honary and Orafai, 2002). The measurements were performed using a 5 kg load cell, a gauge length of 5 cm, and a cross-head speed of 0.2 mm/s. The maximum force at break divided by cross-section area (F/A) was the tensile strength of the films. The ratio of the increase in length ($\Delta L = L - L_0$) to the original length (L_0) was the elongation of the films. Young's modulus (E) of the films can be calculated by using the following equation (Martin, 1993):

$$\frac{F}{A} = E\left(\frac{L - L_0}{L_0}\right) \quad (1)$$

2.3.7. Water uptake and erosion of films

Water uptake and erosion of the films were carried out using gravimetric method. Films were weighed (W_0) and then soaked in 0.1 M HCl that had been incubated at 37.0 ± 0.5 °C and shaken occasionally. After a predetermined time interval, each film was withdrawn, blotted to remove excess water, immediately weighed (W_t), and then dried in a hot air oven at 50 °C to constant weight (W_d). The % water uptake and % erosion can be calculated from the following equation (Tuovinen et al., 2003):

$$\text{water uptake (\%)} = \left(\frac{W_t - W_d}{W_d}\right) \times 100 \quad (2)$$

$$\text{erosion (\%)} = \left(\frac{W_0 - W_d}{W_0}\right) \times 100 \quad (3)$$

where W_0, W_t and W_d are the original, wet and dry weight of the films, respectively.

2.3.8. Water vapor permeability of films

Water vapor permeation (WVP) across the films was studied following the method of Remuñán-López and Bodmeier (1997). Discs were punched from the films, placed on open 5 ml glass vials containing 3.5 g silica gel beads and held in place with a screw lid having a 0.86 cm-diameter of test area (0.58 cm^2). The vials were placed in a dessiccator containing a saturated aqueous sodium chloride solution (75% RH) (Nyqvist, 1983). The dessiccator was kept in a room at 26.0 ± 1.0 °C, 55 ± 3% RH. The weight change was recorded periodically over 72 h. The WVP rate was obtained from the slope of relationship between the amount of water permeated and time. The WVP coefficient of the films was calculated using the following equation (Porter and Ridgway, 1982; Limmatvapirat et al., 2004):

$$\text{WVP coefficient} = \frac{Mh}{A\Delta P_v} \quad (4)$$

where M is the WVP rate, h is the mean thickness of the film, A is the area of the exposed film, and ΔP_v is the vapor pressure difference.

2.3.9. Drug permeability of films

Permeability studies of acetaminophen (ACT) and propranolol HCl (PPN) through the films were performed using a horizontal side-bi-side diffusion cell (Crown Glass Co., Inc., Somerville, NJ) at 37.0 ± 0.5 °C. The films were clamped between donor and receptor compartments of 3 ml volume and the diffusional area was 0.66 cm^2. ACT (4 mg/ml) solution in 0.1 M HCl was placed in the donor compartment, while the receptor compartment was 3 ml of 0.1 M HCl. Both compartments were stirred continuously throughout the tests. At appropriate intervals, 2.5 ml aliquots of the receptor medium were withdrawn and immediately replaced with fresh medium. The amount of ACT was analyzed using UV–vis spectrophotometer at 265 nm (Shimadzu UV1201, Japan).

Drug permeation through a polymeric film was characterized under steady state conditions by means of Fick's first law, which can be expressed as (Martin, 1993; Pokharkar and Sivaram, 1996):

$$\frac{dQ}{A\,dt} = PC_0 \quad (5)$$

where $dQ/A\,dt$ is the permeation flux which is the slope value calculated using linear regression analysis of the linear relationship between the amount of drug permeated and time, A is the surface area of the film which the diffusion is taking place, C_0 is the concentration of drug in the donor compartment which is assumed a constant throughout the test, and P is permeability coefficient. The apparent diffusion coefficient (D) can be estimated using the following equation.

$$t_L = \frac{h^2}{6D} \quad (6)$$

where t_L is the lag time which obtained from the x-intercept of the permeation profiles, and h is the mean thickness of the films. Thus, the apparent partition coefficient (K) is obtained as follows:

$$K = \frac{Ph}{D} \quad (7)$$

2.4. Statistical analysis

One-way analysis of variance (ANOVA) with the least significant difference (LSD) test for multiple comparisons was performed using SPSS program for MS Windows, release 11.5 (SPSS Inc., Chicago, IL) to assess statistical significance on mechanical property, water uptake, erosion and permeability data of the microcomposite films. The significance of the difference was determined at 95% confident limit ($\alpha = 0.5$) and considered to be significant at a level of P less than 0.05.

3. Results and discussion

3.1. Appearance and thickness of the films

SA and composite films were prepared using casting/solvent evaporation method. The transparent SA films were obtained, whereas incorporating MAS gave opaque composite films. Surface morphology and internal structure of the SA films, which the film thickness was 45.3 ± 1.8 μm ($n = 10$), and the composite films were compared using SEM. Smooth surface and dense

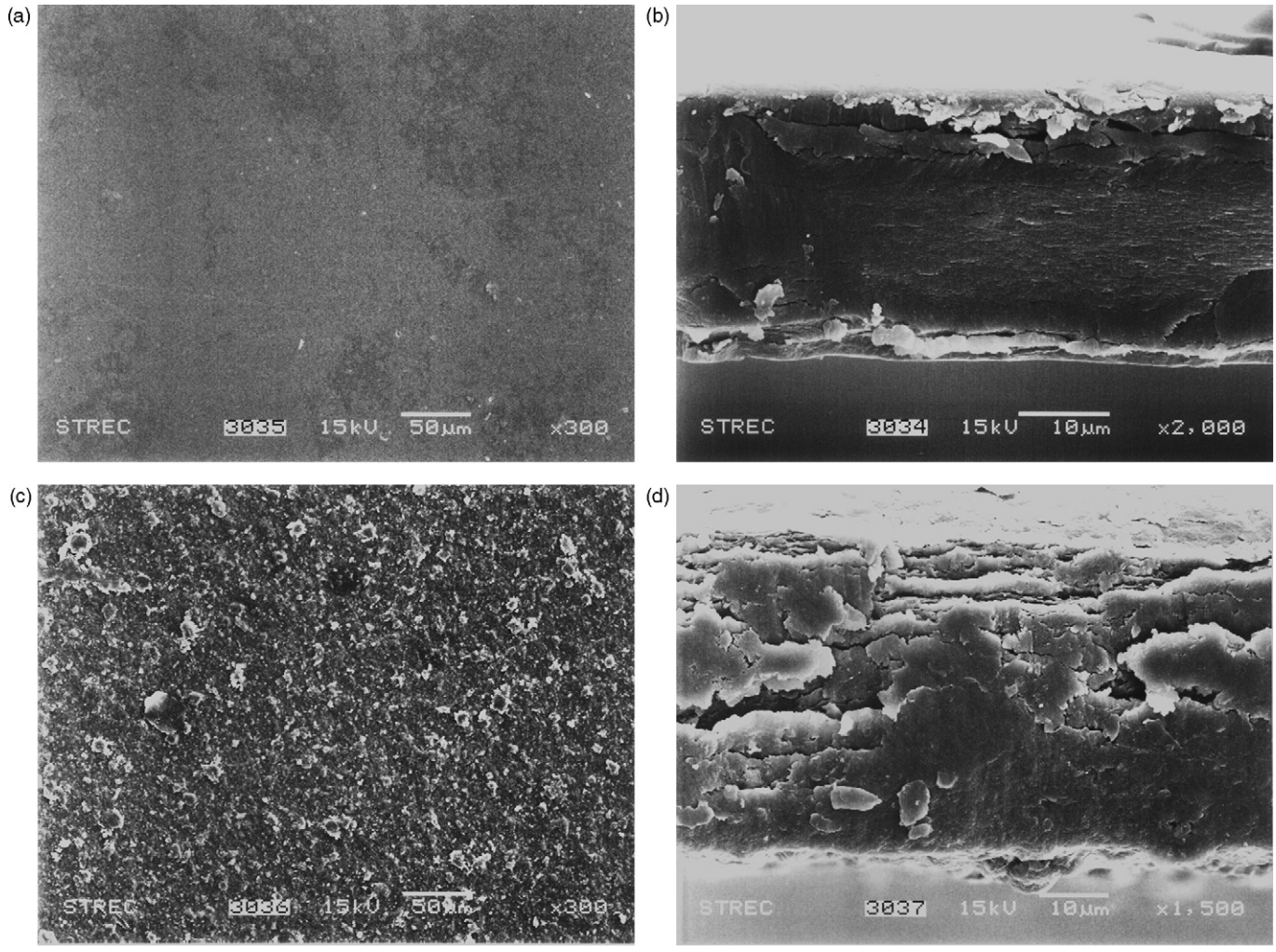

Fig. 1. Surface morphology and cross section of SA film (a and b) and SA–MAS microcomposite film (c and d).

internal structure of the SA film were observed (Fig. 1a and b). In contrast, the composite films had rough surface (Fig. 1c) and layer structure (Fig. 1d). This may be a result of interaction of SA with MAS and recrystallization of MAS (Pongjanyakul et al., 2005b). Although the composite films had looser matrix structure than the SA films, but the composite films were stronger and more flexible than the SA films (Pongjanyakul et al., 2005b).

The thickness of the composite films is shown in Table 1. The dry and wet thickness of the composite films increased remarkably with increasing volume of the composite dispersion used. The percentage of thickness increased after hydration in diluted HCl of all composite films was found to be 104–119% and significant effect of thickness on film hydration was not observed. This indicated a swelling property of this composite film in acidic medium. Moreover, not only dry thickness but also wet thickness showed good linear correlation with solid content in composite dispersion used (Fig. 2). This suggested that the film thickness was directly dependent on solid content in composite dispersion.

3.2. Thermal behavior of the films

DSC thermograms of the composite films are presented in Fig. 3. All films showed broad endothermic peaks around 50–70 °C, indicating a dehydration of water residue. The SA film showed an exothermic peak at about 220 °C and followed with

Table 1
Dry and wet thickness of SA–MAS microcomposite films

Volume of SA–MAS dispersion (ml)	Dry thickness[a] (µm)	Wet thickness[a] (µm)	Thickness increased after hydration[b] (%)
100	37.1 ± 3.3	80.8 ± 5.9	117.8
200	78.0 ± 1.1	159.4 ± 4.2	104.4
300	120.5 ± 2.8	263.8 ± 9.6	118.9

[a] Data are the mean ± S.D., $n = 10$.
[b] ((Mean wet thickness − mean dry thickness)/mean dry thickness) × 100.

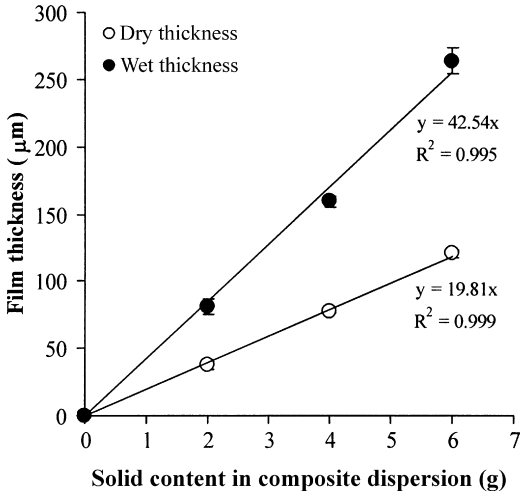

Fig. 2. Relationship between solid content in composite dispersion and film thickness of SA–MAS microcomposite films. Each point is the mean ± S.D., $n = 10$.

an endothermic peak at about 224 °C, and an exothermic decomposition peak around 250 °C (Fig. 3b). The exothermic followed by the endothermic peak of the SA films may be attributable to recrystallization and a phase transition of SA after heat induction (Pongjanyakul et al., 2005b). These peaks shifted to lower temperature in the composite films. The increase in the thickness of the composite films caused these peaks shift to lower temperature. In addition, the exothermic decomposition peaks of the composite films showed lower intensity and higher temperature than that of the SA films. This decomposition peak of the composite films shifted to lower temperature when the film thickness was increased.

The weight loss profile of the films at higher temperature was also studied using TGA. The loss of weight in the SA film at around 220–280 °C indicated a decomposition of SA (Fig. 4b). At higher temperature the SA film showed a high weight loss at around 610–640 °C due to combustion of the residues. MAS showed a weight loss around 30–80 °C that correspond to the loss of surface and interlayer water. Moreover, the weight of MAS slight reduced at temperature higher than 500 °C (Fig. 4a). This was due to dehydroxylation of the MAS sheets (Grim,

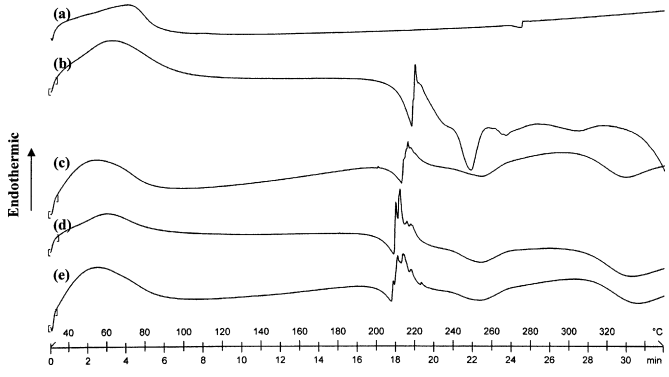

Fig. 3. DSC thermograms of MAS (a), SA film (b), and SA–MAS microcomposite films with different dry thickness of 37.1 μm (c), 78.0 μm (d) and 120.5 μm (e).

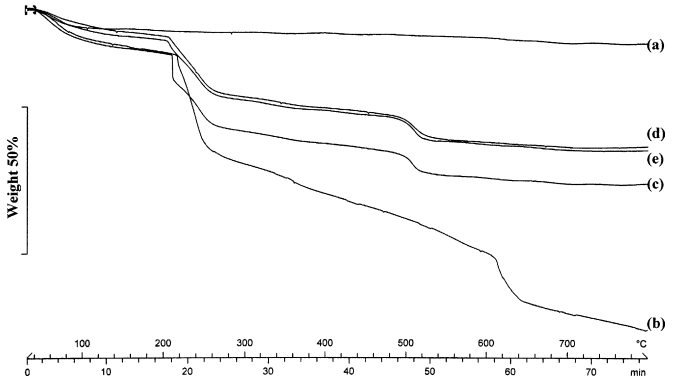

Fig. 4. Weight loss profiles of MAS (a), SA film (b), and SA–MAS microcomposite films with different dry thickness of 37.1 μm (c), 78.0 μm (d) and 120.5 μm (e).

1953). The total weight loss of MAS was about 12% at 800 °C. In the case of the composite films, the weight loss at around 210–260 °C was a decomposition of the composite films, but the percent weight loss of the composite films was obviously lower than that of the SA films. This was because of incorporation of MAS into the films. However, the composite film with 37.1 μm thickness gave higher wt% loss than that with 78.0 and 120.5 μm thicknesses at this temperature (Fig. 4c and d). After that, the composite films had weight loss again at around 500–520 °C. It can be seen that the combustion of the residues of the composite films occurred at lower temperature when compared with the SA films because the dehydroxylation of MAS at this temperature may induce the combustion of the composite films. The thermal properties of the composite films found using DSC and TGA suggested that the film thickness affected thermal behavior of the composite films, indicating that the matrix structure of the films may be changed in the preparation process although the thickness of the composite films correlated with the solid content of dispersion used.

3.3. Crystallinity of the films

The crystallinity of the films was investigated using X-ray diffractometry. The SA film presented an amorphous form with a broad peak at 14°(2θ) (Fig. 5a). MAS powder showed a diffraction peak at approximately 7.1°(2θ), 19.9°(2θ), 22.0°(2θ), and 28.7°(2θ), indicating a crystalline form (Fig. 5b). When compared with MAS and SA films, the composite films showed a different diffraction pattern with peaks at approximately 7.0, 14.3, 21.9 and 28.5°(2θ) (Fig. 5c and d), suggesting a change in crystallinity of the films. Similarity of XRD patterns of the composite films with various thicknesses was found. The basal spacing peak at 7°(2θ) of MAS, represented the thickness of silicate layer (1.2 nm) (Darder et al., 2003; Wang et al., 2005), did not change in the composite films but increased in intensity, indicating that MAS could form higher crystallinity by reaggregation of silicate layers during drying process (Ogata et al., 1997; Lagaly, 1999). However, it can be observed that the basal spacing peak of the thinnest film presented stronger intensity than those of the thicker films, resulting in a higher crystallinity of the films.

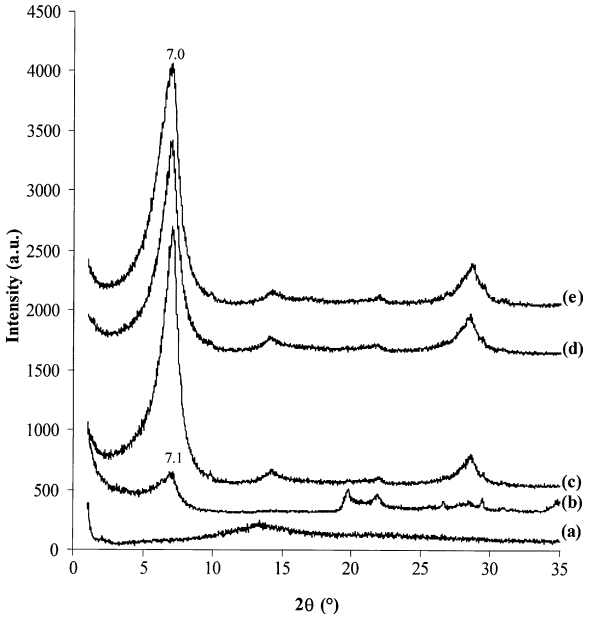

Fig. 5. PXRD patterns of MAS (a), SA film (b), and SA–MAS microcomposite films with different dry thickness of 37.1 μm (c), 78.0 μm (d) and 120.5 μm (e).

The film thickness could affect crystallinity of the films due to the different condition of drying process. Jansson and Thuvander (2004) suggested that fast water evaporation in case of the thin films caused a limitation of molecular movement in the film, whereas slower water evaporation provided enough time for molecules to have relaxation. Since the thick films were exposed to a greater degree of water for a longer time, the crystallinity of the thick films were expected to be higher than the thin films. This expectation was not in agreement with the findings in this study. It can be explained that the fast evaporation of water in the composite dispersion might induce rapid reaggregation of MAS, although MAS could interact with SA in the composite dispersions. This might lead to higher crystallinity of the thinner films.

3.4. Mechanical properties of the films

The mechanical properties of the microcomposite films are presented in Table 2. The tensile strength of the films with 78.0 and 120.5 μm thickness statistically decreased ($P < 0.05$) when compared with that of the films with 37.1 μm dry thickness, whereas the elongation of the 78.0 and 120.5 μm thickness films was significantly higher ($P < 0.05$) than that of the 37.1 μm thickness films. Both parameters affected Young's modulus of the films, which was obviously decreased when the film thickness increased. This indicated that the thin films were stronger than the thick films, which may be due to higher crystallinity of the thin films. The results were in agreement with the previous report in the case of polymer films (Ononokpono and Spring, 1988; Jansson and Thuvander, 2004). The decrease in strength with increasing film thickness could be described that the film surface formed on drying had different properties from the film bulk, and the film surface had higher Young's modulus than the film bulk. The ratio of the depth of the surface layer to film thickness increased with decrease in film thickness. Thus, Young's modulus of the film bulk increased when the film thickness was decreased (Ononokpono and Spring, 1988).

Table 2
Effect of film thickness on mechanical properties of SA–MAS microcomposite films

Dry film thickness (μm)	Tensile strength (MPa)	Elongation (%)	Young's modulus (MPa)
37.1	89.2 ± 6.4	3.3 ± 0.9	2.843.3 ± 627.6
78.0	80.2 ± 3.1	5.0 ± 0.3	1.610.0 ± 84.1
120.5	76.5 ± 7.6	5.5 ± 1.4	1.456.5 ± 283.0

Data are the mean ± S.D., $n = 4$.

3.5. Water uptake and erosion of the films

The percent water uptake in 0.1 M HCl of the films is shown in Fig. 6a. The water uptake of the thinnest films reached an equilibrium in 10 min, whereas the thicker films used a longer time (30 min). A faster water uptake was found in the thinnest

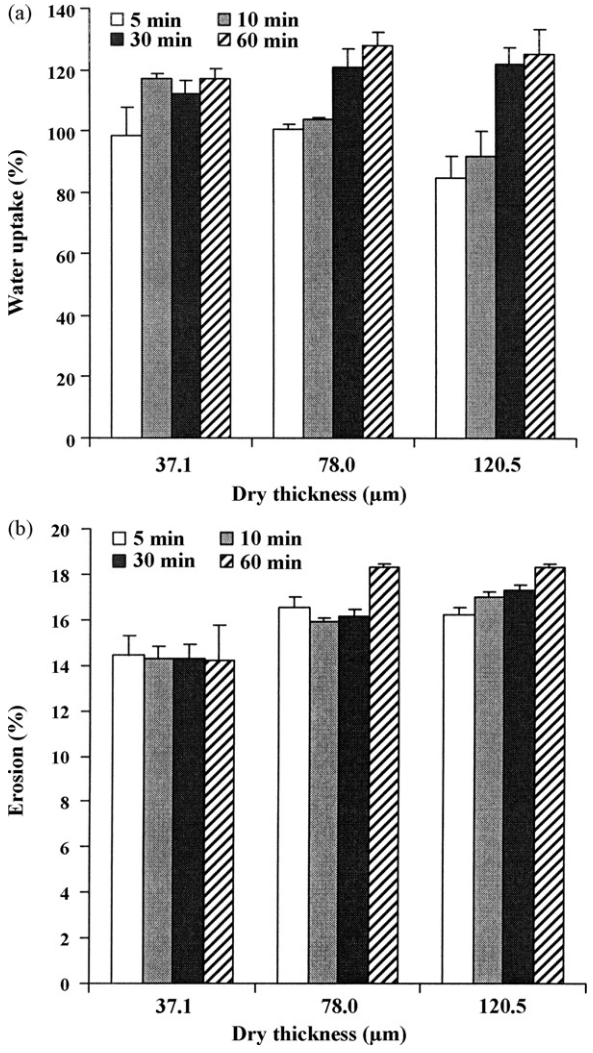

Fig. 6. Effect of dry thickness of microcomposite films on water uptake (a) and erosion (b) in 0.1 M HCl. Each bar is the mean ± S.D., $n = 4$.

film. The thicker films (78.0 and 120.5 μm) provided statistically higher water uptake at 60 min ($P < 0.05$) than the thinnest films. The erosion of the films was also investigated in this study as shown in Fig. 6b. The erosion of the thinnest films was significantly lower ($P < 0.05$) than the thicker films (78.0 and 120.5 μm).

The water uptake and erosion of the composite films could be determined in acidic medium because SA was rapidly changed to water-insoluble alginic acid (Østberg et al., 1994) and in situ insoluble films were formed. Other media, distilled water and phosphate buffer at neutral pH, could not measured these parameters due to a rapid swelling and dissolution of the films. Increasing in water uptake of the thick films suggested that the higher water-filled channels in the matrix structure were created. This indicated that the thick films had a loosen matrix structure when compared with the thin films. An erosion of the composite films took place because of dissolution of some SA on the surface of the films and some water-soluble substances of MAS. The % erosion of the thick films increased because water-soluble substances could easily diffuse out of the films, which possessed loosen matrix structure. Moreover, higher erosion of the thick films was one of the reasons to explain the increase in water uptake.

3.6. Permeability of the films

The effect of film thickness on water vapor permeation (WVP) is presented in Fig. 7a. Relationship between the amount of water vapor permeated and time showed a linear line over 72 h of the test and the slope of this relationship was WVP rate. The WVP rate significantly decreased ($P < 0.05$) with increasing film thickness (Fig. 7b). This is likely to be due to the increase in the diffusion path length of the thick films. However, the WVP rate did not represent the permeability of the films, so water vapor permeability (WVP) coefficient, calculated using Eq. (4), was used for comparison. WVP coefficient statistically increased ($P < 0.05$) with increasing film thickness as shown in Fig. 7b. It can be seen that the different results of WVP rate and WVP coefficient were found when increasing the film thickness. This indicated that the higher water vapor permeability of the thick film was found when compared with the thin films. This also suggested the different matrix structure of the films, which the thick films had looser matrix structure than the thin films.

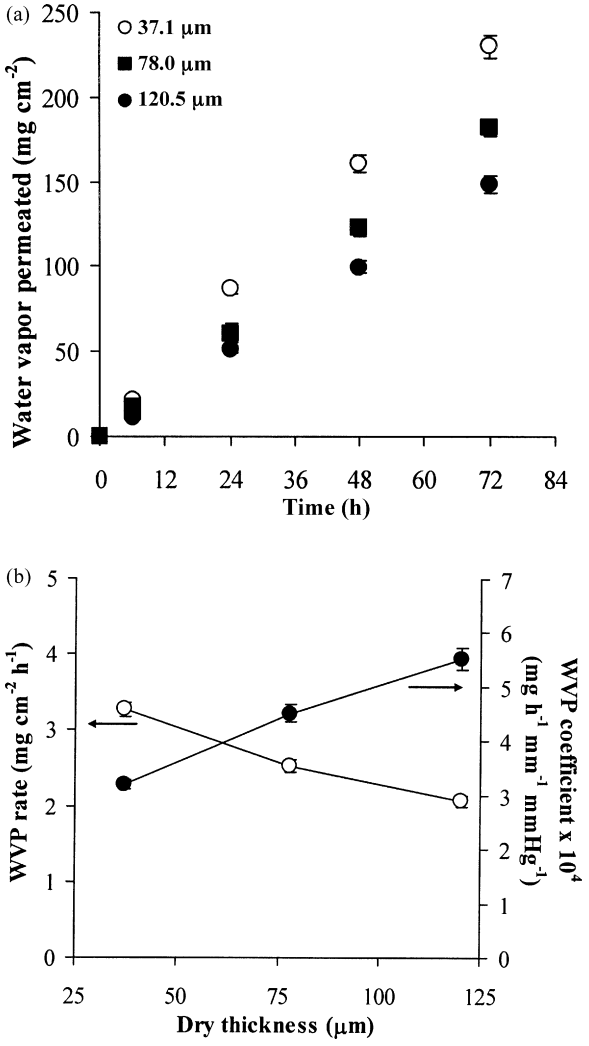

Fig. 7. Effect of dry thickness of microcomposite films on water vapor permeation profiles (a), and relationship between dry thickness and WVP rate and WVP coefficient (b). Each point is the mean ± S.D., $n = 3$.

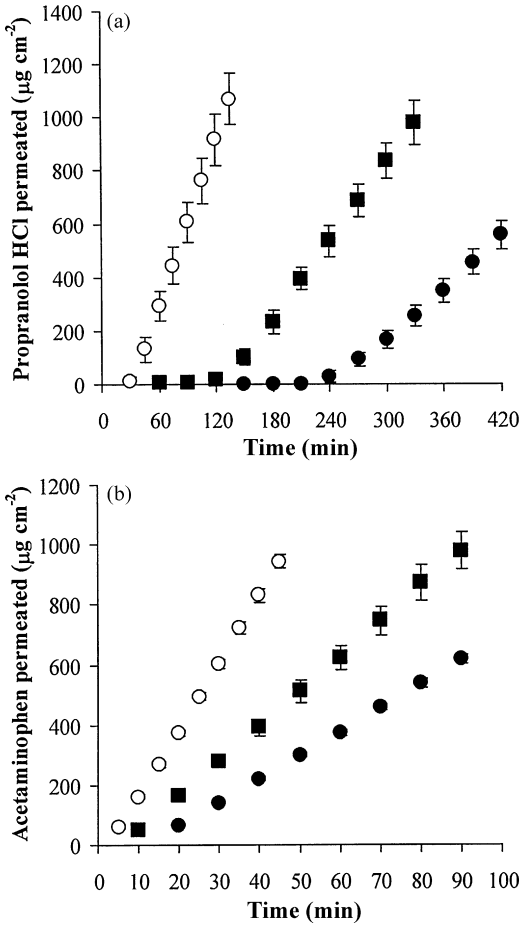

Fig. 8. Permeation profiles of propranolol HCl (a) and acetaminophen (b) across microcomposite films with different wet thicknesses of 80.8 μm (◯), 159.4 μm (■), and 263.8 μm (●). Each point is the mean ± S.D., $n = 3$.

Drug permeability through the films in acidic medium was also studied using propranolol hydrochloride (PPN) and acetaminophen (ACT) as model drugs. The permeation profiles of PPN and ACT across the composite films with various wet thicknesses showed a straight line with a lag time, indicating that the drug permeation reached steady state (Fig. 8). The lag time significantly increased ($P < 0.05$) with increasing wet thickness of the films (Fig. 9a). A shorter lag time was observed when ACT was used. Increasing the wet thickness caused a statistically decreased ($P < 0.05$) of permeability coefficient (P) value of both drugs (Fig. 9b). To compare the permeation of drug through the films without the effect of the thickness of the films, the apparent diffusion coefficient (D) values were estimated using Eq. (6). The D values of both drugs remarkably increased with increasing wet thickness of the films and ACT gave a higher D value than PPN (Fig. 9c). The apparent partition coefficient (K) of both drugs computed using Eq. (7) tended to decrease when wet thickness of the films was increased. A greater K value of PPN was found when compared with ACT (Fig. 9d).

Increasing the wet film thickness provided higher lag time and lower P values of both drugs because of a longer path length of diffusion in the films. Thus the D value was a good parameter for comparing the effect of film thickness. It can be seen that the greater the wet film thickness, the higher the D values were found. It was indicated that the thick films provided a higher water-filled channels and film matrix tortuosity was decreased, resulting in a higher of the D values of both drugs. This suggested a different matrix structure of the films with various thicknesses when exposed with acidic medium.

The effect of different types of drug on permeation across the composite films was also found in this study. PPN (MW = 295.8) had a larger molecule than ACT (MW = 151.16), thus PPN had lower diffusion mobility resulting in a lower D value. Moreover, PPN, which had a pK_a of 9.5, could be ionized in acid medium to produce positive charge molecules, which was strongly adsorbed into the interlayer space of MAS (Matrin et al., 1981). The led to a longer lag time and higher K value for permeation through the films. ACT a weak acid and non-electrolyte with pK_a value between 9.5 and 9.9, so the ionization of ACT in acid medium is very low and is not observed (Nakano et al., 1984; Terzyk et al., 2003). Thus the less adsorption of ACT on MAS was obtained. Moreover, the K values seemed to decrease with increasing wet film thickness because the thick film possessed an increase in hydrophilic properties due to higher water-filled channel in the matrix structure, leading to a less affinity of drugs on the films.

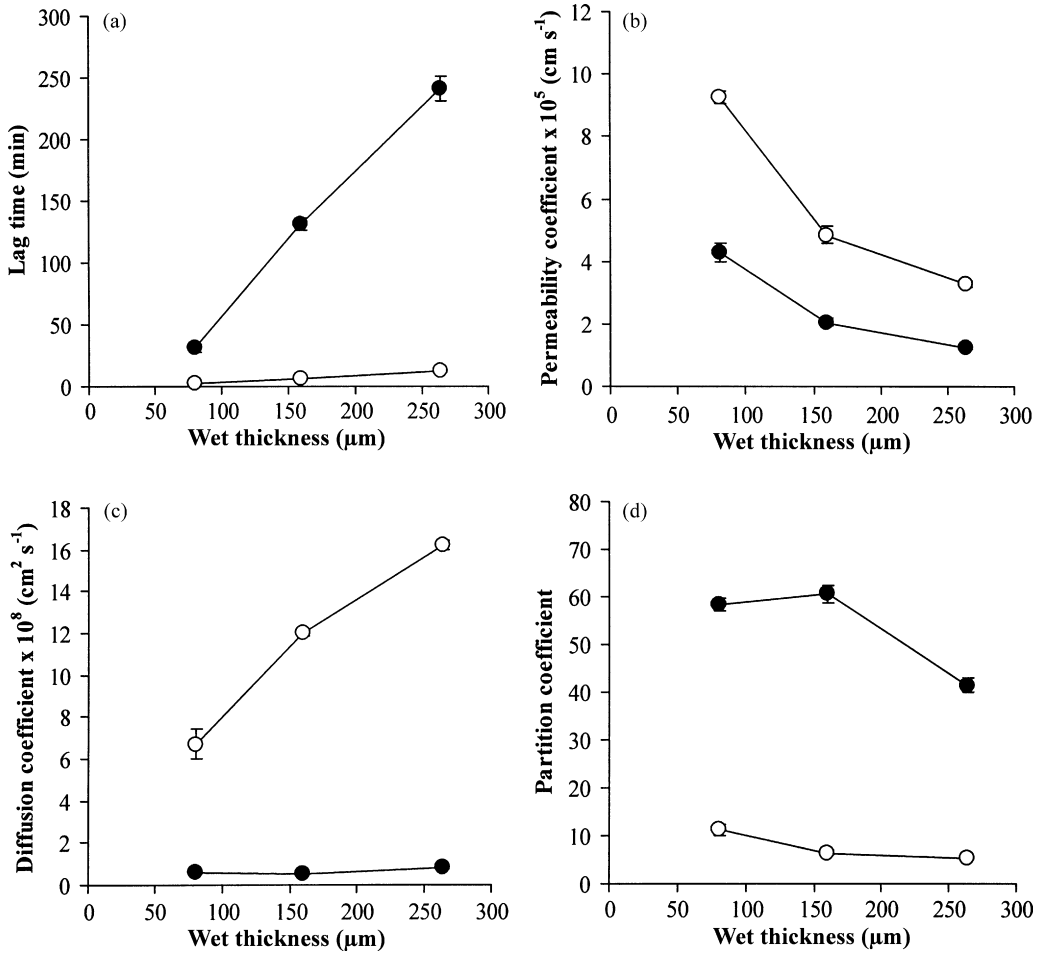

Fig. 9. Effect of wet film thickness on lag time (a), permeability coefficient (b), diffusion coefficient (c), and partition coefficient (d) of acetaminophen (◯) and propranolol HCl (●). Each point is the mean ± S.D., $n = 3$.

4. Conclusion

The different thicknesses of the SA–MAS microcomposite films can be prepared by varying volumes of the composite dispersion for casting and then using solvent evaporation method for drying. The evaporation rate of solvent in different volumes used could affect crystallinity of the microcomposite films and strength of the film surface and film bulk. The higher the film thickness, the weaker the film bulk was obtained. This was resulted from a loose matrix structure of the thick films. Consequently, the water uptake and erosion, as well as the water vapor and drug permeability of the thick films were higher than those of the thin films. The findings suggest that the film thicknesses of the SA–MAS microcomposite films prepared by varying volumes of the composite dispersion for casting could influence crystallinity, mechanical properties, water absorption and film permeability.

Acknowledgments

The authors wish to thank Commission on Higher Education, Ministry of Education (Bangkok, Thailand) and the Thailand Research Fund (Bangkok, Thailand) for financial support (Grant no. RMU4980022). We also thank to Faculty of Pharmaceutical Sciences, Khon Kaen University (Khon Kaen, Thailand) and Faculty of Pharmacy, Mahidol University (Bangkok, Thailand) for technical supports.

References

Alexandre, M., Dubois, P., 2000. Polymer-layered silicate nanocomposites: preparation, properties and uses of a new class of materials. Mater. Sci. Eng. 28, 1–63.

American Society for testing and Material (ASTM) D 882, 2002. Standard test methods for tensile properties of thin plastic sheeting, Annual Book of ASTM Standards, vol. 06.01. ASTM International, West Conshohocken, pp. 164–173.

Aslani, P., Kennedy, R.A., 1996. Studies on diffusion in alginate gels. I. Effect of cross-linking with calcium or zinc ions on diffusion of acetaminophen. J. Control. Release 42, 75–82.

Badwan, A.A., Abumalooh, A., Sallam, E., Abukalaf, A., Jawan, O., 1985. A sustained release drug delivery system using calcium alginate beads. Drug Dev. Ind. Pharm. 11, 239–256.

Ciullo, P.A., 1981. Rheological properties of magnesium aluminum silicate/xanthan gum dispersions. J. Soc. Cosmet. Chem. 32, 275–285.

Ciullo, P.A., Braun, D.B., 1991. Clay/carbomer mixtures enhance emulsion stability. Cosmet. Toilet. 106, 89–95.

Darder, M., Colilla, M., Ruiz-Hitzky, E., 2003. Biopolymer–clay nanocomposites based on chitosan intercalated in montmorillonite. Chem. Mater. 15, 3774–3780.

Draget, K.I., 2000. Alginates. In: Philips, G.O., Williams, P.A. (Eds.), Handbook of Hydrocolloids. Woodhead Publishing, Cambridge, pp. 379–395.

Grim, R.E., 1953. Clay Mineralogy. McGraw-Hill Book Company, Inc., New York, pp. 190–249.

Honary, S., Orafai, H., 2002. The effect of different plasticizer molecular weights and concentrations on mechanical and thermomechanical properties of free films. Drug Dev. Ind. Pharm. 28, 711–715.

Jansson, A., Thuvander, F., 2004. Influence of thickness on the mechanical properties for starch films. Carbohydr. Polym. 56, 499–503.

Julian, T.N., Radebaugh, G.W., Wisniewski, S.J., 1988. Permeability characteristics of calcium alginate films. J. Control. Release 8, 165–169.

Kibbe, H.A., 2000. Handbook of Pharmaceutical Excipients, 3rd ed. American Pharmaceutical Association, Washington, pp. 295–298, 465–467.

Lagaly, G., 1999. Introduction: from clay mineral–polymer interaction to clay mineral–polymer nanocomposites. Appl. Clay. Sci. 15, 1–9.

Limmatvapirat, S., Limmatvapirat, C., Luangtana-anan, M., Nuntanid, J., Oguchi, T., Tozuka, Y., Yamamoto, K., Puttipipatkhachorn, S., 2004. Modification of physicochemical and mechanical properties of shellac by partial hydrolysis. Int. J. Pharm. 278, 41–49.

Martin, A., 1993. Physical Pharmacy, 4th ed. Lea & Febiger, Philadelphia, pp. 324–361, 556–594.

Matrin, M.J.S., Camazano, M.S., Hernández, M.T.V., Dominguez-Gil, A., 1981. Interaction of propranolol hydrochloride with montmorillonite. J. Pharm. Pharmacol. 33, 408–410.

McCaig, M.S., Paul, D.R., 2000. Effect of film thickness on the changes in gas permeability of a glassy polyarylate due to physical aging. Part I. Experimental observations. Polymer 41, 629–637.

Nakano, N.I., Shimamori, Y., Umehashi, M., Nakano, M., 1984. Preparation and drug adsorption characteristics of activated carbon beads suitable for oral administration. Chem. Pharm. Bull. 32, 699–707.

Nyqvist, H., 1983. Saturated salt solutions for maintaining specified relative humidities. Int. J. Pharm. Tech. Prod. Manuf. 4, 47–48.

Ogata, N., Kawakage, S., Ogihara, T., 1997. Poly(vinyl alcohol)–clay and poly(ethylene oxide)–clay blends prepared using water as solvent. J. Appl. Polym. Sci. 66, 573–581.

Ononokpono, O.E., Spring, M.S., 1988. The influence of binder film thickness on the mechanical properties of binder films in tension. J. Pharm. Pharmacol. 40, 126–128.

Østberg, T., Lund, E.M., Graffner, C., 1994. Calcium alginate matrices for oral multiple unit administration. IV. Release characteristics in different media. Int. J. Pharm. 112, 241–248.

Pokharkar, V.B., Sivaram, S., 1996. Permeability studies across poly(alkylene carbonate) membranes. J. Control. Release 41, 157–162.

Pongjanyakul, T., Priprem, A., Puttipipatkhachorn, S., 2005a. Influence of magnesium aluminium silicate on rheological, release and permeation characteristics of diclofenac sodium aqueous gels in vitro. J. Pharm. Pharmacol. 57, 429–434.

Pongjanyakul, T., Priprem, A., Puttipipatkhachorn, S., 2005b. Investigation of novel alginate–magnesium aluminum silicate microcomposite films for modified-release tablets. J. Control. Release 107, 343–356.

Pongjanyakul, T., Puttipipatkhachorn, S., 2007. Alginate-magnesium aluminum silicate films: effect of plasticizers on film properties, drug permeation and drug release from coated tablets. Int. J. Pharm. 333, 34–44.

Porter, S.C., Ridgway, K., 1982. The permeability of enteric coatings and the dissolution rates of coated tablets. J. Pharm. Pharmacol. 34, 5–8.

Remuñán-López, C., Bodmeier, R., 1997. Mechanical, water uptake and permeability properties of crosslinked chitosan glutamate and alginate films. J. Control. Release 44, 215–225.

Shishatskii, A.M., Yampol'skii, Y.P., Peinemann, K.V., 1996. Effects of film thickness on density and gas permeation parameters of glassy polymers. J. Membr. Sci. 112, 275–285.

Sugawara, S., Imai, T., Otagiri, M., 1994. The controlled release of prenisolone using alginate gel. Pharm. Res. 11, 272–277.

Takka, S., Ocak, Ö.H., Acartürk, F., 1998. Formulation and investigation of nicardipine HCl–alginate gel beads with factorial design-based studies. Eur. J. Pharm. Sci. 6, 241–246.

Terzyk, A.P., Rychlicki, G., Biniak, S., Łukaszewicz, J.P., 2003. New correlations between the composition of the surface layer of carbon and its physicochemical properties exposed while paracetamol is adsorbed at different temperature and pH. J. Colloid Interface Sci. 257, 13–30.

Tuovinen, L., Peltonen, S., Järvinen, K., 2003. Drug release from starch–acetate films. J. Control. Release 91, 345–354.

Wang, S.F., Shen, L., Tong, Y.J., Chen, L., Phang, I.Y., Lim, P.Q., Liu, T.X., 2005. Biopolymer chitosan/montmorillonite nanocomposites: preparation and characterization. Polym. Degrad. Stab. 90, 123–131.

Zatz, J.L., Kushla, G.P., 1989. Gels. In: Lieberman, H.A., Rieger, M.M., Banker, G.S. (Eds.), Pharmaceutical Dosage Forms: Disperse Systems, vol. 19. Marcel Dekker, New York and Basel, pp. 495–510.